



DIFFUSION IN RANDOM MEDIA

By
SOLOMON NEGASH ASFAW

SUBMITTED IN PARTIAL FULFILLMENT OF THE
REQUIREMENTS FOR THE DEGREE OF
MASTER OF SCIENCE IN PHYSICS

AT
ADDIS ABABA UNIVERSITY
ADDIS ABABA, ETHIOPIA

JUNE 2010

ADDIS ABABA UNIVERSITY
DEPARTMENT OF
PHYSICS

Supervisor:

Dr. TATEK YERGOU

Examiners:

Dr. MESFIN TSIKE

Dr. LEMI DEMEYU

ADDIS ABABA UNIVERSITY

Date: **JUNE 2010**

Author: **SOLOMON NEGASH ASFAW**

Title: **DIFFUSION IN RANDOM MEDIA**

Department: **Physics**

Degree: **M.Sc.** Convocation: **JUNE** Year: **2010**

Permission is herewith granted to Addis Ababa University to circulate and to have copied for non-commercial purposes, at its discretion, the above title upon the request of individuals or institutions.

Signature of Author

THE AUTHOR RESERVES OTHER PUBLICATION RIGHTS, AND NEITHER THE THESIS NOR EXTENSIVE EXTRACTS FROM IT MAY BE PRINTED OR OTHERWISE REPRODUCED WITHOUT THE AUTHOR'S WRITTEN PERMISSION.

THE AUTHOR ATTESTS THAT PERMISSION HAS BEEN OBTAINED FOR THE USE OF ANY COPYRIGHTED MATERIAL APPEARING IN THIS THESIS (OTHER THAN BRIEF EXCERPTS REQUIRING ONLY PROPER ACKNOWLEDGEMENT IN SCHOLARLY WRITING) AND THAT ALL SUCH USE IS CLEARLY ACKNOWLEDGED.

Table of Contents

Table of Contents	iv
List of Figures	v
Abstract	viii
Acknowledgements	ix
1 Introduction	1
1.1 Particle diffusion	1
1.1.1 Normal diffusion	3
1.1.2 Anomalous diffusion	5
1.2 Polymer diffusion	7
2 Methods	14
2.1 Particle diffusion	14
2.2 Polymer diffusion	17
3 Results and discussion	20
3.1 Particle diffusion	20
3.1.1 Plots of mean-square displacement	20
3.1.2 The concentration dependence of d_w	24
3.1.3 The concentration dependence of D	25
3.2 Polymer diffusion	27
3.2.1 Static properties	27
3.2.2 Dynamic properties	29
4 Summary and conclusion	35
Bibliography	37

List of Figures

2.1	Square lattice: among the four nearest-neighbor sites the possible jump directions of the tracer (red) is indicated by the arrows (i.e up,down and left). To the right it is not possible for the tracer to jump because it is occupied by an obstacle (black).	15
2.2	Hexagonal lattice: a single lattice site having six nearest-neighbors. The tracer at the center (red) only jumps to three free lattice sites as indicated by the arrows. Since the rest are blocked by the point obstacles (black). . .	15
2.3	Diffusion of a tracer with periodic boundary conditions. Sites that are connected by the dotted lines that wrap around the lattice are considered to be nearest neighbors and thus a tracer can jump to the opposite edge of the lattice.	16
2.4	Illustration of the bond fluctuation method. The typical moves are indicated. The bond length l varies between 2 and $\sqrt{13}$. From the diagram we can see from left to right the distance between the first and the second is $\sqrt{10}$ and if we continue up to the last (six) monomers respectively we have the distances $\sqrt{5}$, $\sqrt{8}$, 2 and 3.	19
3.1	Mean-square displacement $\langle r^2 \rangle$ as a function of time t for diffusion of a point tracer on a square lattice in the presence of point obstacles at the indicated obstacle concentrations C	20
3.2	The same data re-plotted as the logarithm of the means-quare displacement $\log(\langle r^2 \rangle)$ as a function of the logarithm of time $\log t$. Again, the slight change in slope with time is evident for $C \geq 0.3$	21

3.3	Diffusion of the tracer on a 2D square lattice in which the same data re-plotted as $\log\langle r^2 \rangle / t$ as a function of $\log t$ to obtain the clear picture of time dependence.	22
3.4	Diffusion of a tracer on a 2D hexagonal lattice which shows the time dependence of diffusion when $\log\langle r^2 \rangle / t$ as a function of $\log t$ is plotted. The percolation threshold is 0.6 in which diffusion is anomalous for all times.	23
3.5	Anomalous diffusion exponent d_w as a function of obstacle concentration C for two different geometries: point obstacles on the square lattice (SQ) and point obstacles on a hexagonal lattice (HEX). At the percolation threshold $C = C_p$. Where $C_p = 0.4$ for square lattice and $C_p = 0.6$ for hexagonal lattice.	24
3.6	Anomalous diffusion exponent as a function of C/C_p , the value of the percolation threshold is $C_p = 0.4$ for square lattice and $C_p = 0.6$ for hexagonal lattice.	25
3.7	Diffusion coefficients D as a function of obstacle concentration C for point obstacles on the square lattice.	26
3.8	Log-log plot of end-to-end distance $\langle R^2(N) \rangle$ versus chain length N for self-avoiding walk, $\langle R^2(N) \rangle \propto N^{3/2}$. The chain length or the number of monomer considered are $N = 54, 100, 200$	27
3.9	Log-log plot of radius of gyration $\langle R_g^2(N) \rangle$ versus chain length N for a self-avoiding walk, $\langle R_g^2(N) \rangle \propto N^{3/2}$. The chain length or the number of monomer considered are $N = 54, 100, 200$	29
3.10	Plot of the mean-square displacement of the center of mass of a polymer $g_3(t)$ as a function of Monte Carlo time steps (a) for $C = 0.0$ and (b) for $C=0.35$ concentration of obstacles.	30
3.11	Plot of the mean-square displacement of the center of mass of a polymer $g_3(t)$ as a function of Monte Carlo time steps for a concentrations between $C = 0.0$ and $C = 0.7$	31
3.12	Diffusion coefficient $D = \lim_{t \rightarrow \infty} g_3(t)/t$ as a function of obstacle concentration for a chain length of $N = 20$ monomers.	32
3.13	Diffusion coefficient $D = \lim_{t \rightarrow \infty} g_3(t)/t$ versus number of monomers $N = 20, 50, 100$ for zero concentration of obstacles.	33

3.14 Mean-square displacement $g_1(t)$ and $g_2(t)$ and the diffusion of the center of mass of the polymer $g_3(t)$ (a) for $C = 0.0$ and (b) for $C = 0.2$ and $N = 20$ as a function of Monte Carlo time step. For calculation of this point 100 independent runs are taken into account. 34

Abstract

In this work we present Monte Carlo simulations of particle and polymer diffusion in two dimensional (2D) media with obstacles distributed randomly. For diffusion of a particle, the mean-square displacement of the diffusing species is proportional to time for normal diffusion. But in disordered systems anomalous diffusion may occur, in which the mean-square displacement is proportional to some other power of time. In the presence of moderate concentration of obstacles, diffusion is anomalous for short times and normal for long times. Monte Carlo calculations are used to characterize anomalous diffusion for obstacle concentrations between zero and the percolation threshold. As the obstacle concentration approaches the percolation threshold, diffusion becomes more anomalous for long times; the anomalous diffusion exponent increases. In polymer diffusion, we present a new effective algorithm to simulate dynamic properties of polymeric systems confined to lattice. The algorithm displays Rouse behavior for all spatial dimensions. The systems are simulated by bond fluctuation method to study both the static and dynamic properties of the polymer chains. For static properties we calculated the average mean-square end-to-end distance $\langle R^2(N) \rangle$ and the mean-square radius of gyration $\langle R_g^2(N) \rangle$. Both the end-to-end distance and the radius of gyration are proportional to some power of the number of monomers (N), $\langle R^2(N) \rangle \propto N^{3/2}$ and $\langle R_g^2(N) \rangle \propto N^{3/2}$. For dynamical properties we look at the mean-square displacement of the total chain. For short times the mean-square displacement of the monomers $g_1(t)$ and the mean-square displacement of the monomers relative to the chains center of mass $g_2(t)$ show the same behavior and for long times the mean-square displacement of the center of mass $g_3(t)$ takes over.

Acknowledgements

First of all, I would like to thank the almighty; God, for letting me accomplish this work with success.

Secondly my heart felt gratitude goes to Dr.Tatek Yergou , my advisor, for his many suggestions and constant support as well as constructive comment during this research. His tireless follow up and his consistent support will be unforgettable.

In addition my deepest gratitude goes to my family and my colleagues, who supported me through out this work. They are the hero of my success with out their push and support, this stage is unthinkable.

Finally I would especially like to thank my lovely fiancee Liyu Teklu for her unlimited encouragement and support during this work.

Chapter 1

Introduction

1.1 Particle diffusion

Diffusion is the process by which matter is transported from one part of a system to another as a result of random molecular motions. It is usually illustrated by the classical experiment in which a tall cylindrical vessel has its lower part filled with iodine solution, for example, and a column of clear water is poured on top, carefully and slowly, so that no convection currents are set up. At first the colored part is separated from the clear by a sharp, well defined boundary. Later it is found that the upper part becomes colored, the color getting fainter towards the top, while the lower part becomes correspondingly less intensely colored. After sufficient time the whole solution appears uniformly colored. There is evidently, therefore, a transfer of iodine molecules from the lower to the upper part of the vessel taking place in the absence of convection currents. The iodine is said to have diffused into the water.

If it were possible to watch individual molecules of iodine, and this can be done effectively by replacing them by particles small enough to share the molecular motions but just large enough to be visible under the microscope, it would be found that the motion of each molecule is a random one. In a dilute solution each molecule of iodine behaves independently of the others, which it seldom meets, and each is constantly undergoing collision with solvent molecules, as a result of which collisions it moves sometimes towards

a region of higher, sometimes of lower, concentration, having no preferred direction of motion towards one or the other. The motion of a single molecule can be described in terms of the familiar 'random walk' picture, and whilst it is possible to calculate the mean square displacement traveled in a given interval of time it is not possible to say in what direction a given molecule will move in that time. This picture of random molecular motions, in which no molecule has a preferred direction of motion, has to be reconciled with the fact that a transfer of iodine molecules from the region of higher to that of lower concentration is nevertheless observed.

The concepts of diffusion and random walk have helped us to increase our understanding of the movement of molecules in biological, physical and chemical systems. So, diffusion of particles is taught both in physics and chemistry courses, and the subject matter has roots in biology if we think of Adolf Fick or Robert Brown. The scope of applicability of the theory of diffusion is truly limitless. The subject of diffusion within different types of media has been the focus of increasing interest over the past few decades [1,2]. It was initially focused on the movements of small particles in quenched media. Although narrow, this field has increased our knowledge concerning the diffusion of proteins along bio-membranes, the gel electrophoresis of particles for the purpose of separation, and the development of micro-fabricated devices used to separate molecules. In general it plays an essential role in a wide variety of physical and chemical phenomena involving chemical kinetics [3], conductivity [4], glasses [5], cellular media [6,7], etc. A considerable amount of work has been devoted to the study of diffusion in disordered media. In particular, it has been observed that transport properties are highly sensitive to structural changes. However, a complete description of all possible interactions between diffusion and such disorder remains an active area of research, where new phenomena are discovered regularly.

1.1.1 Normal diffusion

Translational diffusion is the movement of a substance from one region of space to another. In a homogeneous solvent where solute size is comparable to or greater than that of the solvent, solute movement is described well by phenomenological or statistical equations in which the primary determinants of diffusion are solute size and shape. We call this type of diffusion normal diffusion. In normal (unobstructed) diffusion, the mean-square displacement of the diffusing particle is proportional to time. This follows directly from the solution to the classical diffusion equation.

The flux of solute, J , through a planar area in space is proportional to the concentration gradient across the plane:

$$J = -D\nabla C. \quad (1.1.1)$$

Where C is the concentration of solute and the operator ∇ represents the derivative of C with respect to spatial coordinates. C is generally a function of both time and space. Requiring mass balance, the diffusion equation becomes

$$\frac{\partial C}{\partial t} = \nabla \cdot (D\nabla C). \quad (1.1.2)$$

Equations (1.1.1) and (1.1.2) are Fick's first and second laws of diffusion, respectively. Solutions to Fick's laws are given by Crank [8]; additional solutions are given by Hines and Maddox [9]. Fick's laws are phenomenological laws that describe the spatial and temporal dissipation of a concentration gradient. The diffusion constant can be concentration dependent, although in practice D is assumed to be constant. For constant D , Fick's second law becomes $\partial C/\partial t = D\nabla^2 C$. Diffusion can also be anisotropic, in which case D becomes a tensor.

In the absence of a concentration gradient, normal diffusion is usually described by Einstein's equations of Brownian motion [10]. For a solute comparable to or larger than

the solvent, the diffusion coefficient is given by:

$$D = kT/f, \quad (1.1.3)$$

Where k is Boltzmann's constant, T is the absolute temperature, and f is the solvent friction coefficient. In normal diffusion, the solvent is usually thought of as a continuous hydrodynamic fluid in which the details of the solvent structure and the solvent-solute interaction are ignored. For a spherical particle in a hydrodynamic solvent of shear viscosity η , the solvent friction coefficient in Equation (1.1.3) is :

$$f = 6\pi\eta r_h, \quad (1.1.4)$$

Where r_h is the hydrodynamic radius of the particle. Equation (1.1.4) corresponds to stick boundary conditions between the solute and solvent in which the hydrodynamic solvent is considered to stick to the solute at the solute-solvent boundary. For slip boundary conditions (no stickiness between the solvent and solute), the factor 6π in Equation (1.1.4) is replaced by 4π . For non-spherical shapes, the friction coefficient is multiplied by a shape factor that is greater than one. From Fick's laws or from Einstein's relations, the mean-squared displacement (MSD) (i.e. the square of the displacement of a particle at some time relative to the position of the particle at zero time, averaged over many particles), $\langle r^2 \rangle$, of a solute particle in three dimensions is related to D by:

$$\langle r^2 \rangle = 6Dt. \quad (1.1.5)$$

For one dimension the MSD is $\langle r^2 \rangle = 2Dt$ and for two dimension it is $\langle r^2 \rangle = 4Dt$. The validity of Equation (1.1.5) for solute diffusion in fluid phases has been demonstrated many times over the past 100 years [11]. The equations of normal diffusion rest upon the central limit theorem: The average displacement of a particle is Gaussian distributed if the displacements themselves have a finite second moment (i.e., a finite squared deviation

from the origin) and are Markovian (i.e., the probability of a particular displacement is independent of previous displacements)[12]. Displacements that do not follow this central limit theorem, such as displacement distributions having long tails that do not approach zero exponentially, or displacement that are correlated, will not in general lead to normal diffusion. These processes lead to anomalous diffusion.

1.1.2 Anomalous diffusion

A central assumption in describing normal solute diffusion is that the solute diffuses in a continuous hydrodynamic fluid. This assumption is clearly not valid in most biological systems. In inhomogeneous environments, or where the solute is smaller than the solvent, or where a large fraction of the solution volume is occupied by another solute (a crowder), more complex equations may be necessary to describe solute movement. We call this type of diffusion in which solute movement is not described by the equations of normal diffusion as anomalous diffusion. A variety of mechanisms lead to anomalous diffusion, involving broad distributions of jump times, broad distributions of jump lengths, or strong correlations in diffusive motion (Bouchaud and Georges, 1988; Bouchaud and Georges, 1990; Scher et al., 1991). For diffusion in cell membranes the relevant mechanisms are obstruction (crowding), which can produce strong correlations, and binding, which can produce a broad distribution of jump times.

The cytoplasm and the aqueous compartments of intracellular organelles such as mitochondria are crowded with small solutes, soluble macromolecules, skeletal proteins, and membranes. Cell membranes are crowded with lipids, some of which are organized into raft structures, and proteins, some of which are tethered to skeletal proteins and contain extensive external appendages. Popular pictorial representations of the aqueous environment within cells [13] suggest that crowding would seriously hinder solute diffusion a major determinant of metabolism, transport phenomena, signaling, and cell motility. One possible consequence of molecular crowding and hindered diffusion is the need for

compartmentalized metabolism to overcome diffusive barriers. A second predicted consequence of molecular crowding is that the physical chemistry of interactions in cells, such as protein-protein associations and enzyme reactions, is drastically altered. So, obstruction and binding hinder diffusion, and the mean-square displacement is proportional to a fractional power of time less than one. Here we consider only obstruction.

In anomalous (obstructed) diffusion the mean-square displacement is proportional to a fractional power of time not equal to one.

$$\langle r^2 \rangle = 4Dt^{2/d_w}, \quad (1.1.6)$$

Where d_w is the anomalous diffusion exponent. If $d_w = 2$, we recover normal diffusion. For obstructed diffusion, $d_w > 2$, and diffusion is slowed down. Equation (1.1.6) is obtained from theoretical arguments and is confirmed by Monte Carlo results (Havlin and Ben-Avraham, 1987; Havlin and Bunde, 1991). At obstacle concentrations below the percolation threshold, diffusion is anomalous at short distances and normal at long distances. In the short time regime, we often find that $\langle r^2 \rangle$ is not a linear function of time because the particle has not had sufficient opportunity to fully explore its surroundings. The phenomenon is even more pronounced when the particle moves in a fractal environment. This is rarely a typical experimental situation, however, since the fractal nature of all real systems are limited both at the small and large length scales. For biophysical applications, we need to consider a wider range of obstacle concentrations, from unobstructed diffusion to the percolation threshold. We shall examine the time over which anomalous diffusion occurs and how large a deviation from normal diffusion occurs. The key quantity in the analysis is the ratio of the mean-square displacement $\langle r^2 \rangle$ to the time t .

Single particle tracking experiments have provided evidence of anomalous diffusion of membrane proteins in cells (Ghosh and Webb, 1990; Ghosh, 1991). The low density lipoprotein (LDL) receptor was labeled with a highly fluorescent form of LDL. Computer enhanced video microscopy was used to track the trajectories of individual receptors as

they moved on the cell surface. The time resolution was $\frac{1}{30}s$ and the spatial resolution was 30nm . The mean-square displacement was calculated by averaging within a single trajectory. In some trajectories, a log-log plot of the mean-square displacement as a function of time showed anomalous diffusion, and transitions between anomalous and normal diffusion were observed.

Anomalous diffusion may be observable in fluorescence photo bleaching recovery experiments as well (Brust-Mascher et al., 1993). When anomalous diffusion occurs, probability density for a diffusing particle is not the usual Gaussian distribution, but a stretched exponential (Klafter et al., 1992), so the form of the fluorescence recovery curve changes. Nagle (1992) has shown for one dimensional systems that long time tails in the jump rate of the diffusing species affect the shape of the photo bleaching recovery curve. If such a recovery curve is analyzed by conventional means, the diffusion coefficient and the fractional recovery depend on the measurement time. Long time tails may result from transient binding of the diffusing species to immobile species, if the distribution of binding energies is wide enough. The approximations in a lattice model of diffusion are summarized elsewhere (Scalettar and Abney, 1991; Saxton, 1993a). For purposes of this paper, the most important limitation of a lattice model is that it gives no information about dynamics on time scales less than the time required for a particle (tracer) to diffuse one lattice constant. For example, we neglect the decay of inertial terms, which takes place on a time scale of $10^{-13}s$ (Abney et al., 1989). Furthermore, hydrodynamic interactions are neglected, and small errors due to the discrete nature of the lattice may appear at distances less than a few lattice constants.

1.2 Polymer diffusion

Polymers are fascinating molecules that are applied and fabricated for virtually all our day-to-day activities. The diversity with which polymers are used these days is truly

staggering. Here we will begin by defining polymers and briefly describe their relevant static and dynamic properties.

From the most general point of view, any plastic or rubber is considered a polymer. Your glasses are likely made of polymers. The "ink" on this page is a polymer. From a scientific point of view the actual definition of a polymer may well depend on whom you ask. A mathematician will tell you that it is a molecule whose form is depicted as a random walk. A chemist will say that a polymer is a series of identical molecules that are covalently bonded to form long chains. A physicist may compare polymers with a fluid containing fewer degrees of freedom. While these descriptions are essentially valid, they each provide only a portion of the answer to our question. By taking each perspective into consideration, we achieve a better understanding of what a polymer is.

So what makes the study of polymers so attractive? Firstly, polymers can both be fabricated or found in nature. DNA molecules, for example, are considered polymers. Secondly, dilute solutions of polymers can be seen as liquids whose molecules are not strongly correlated to their neighbors. This makes their study far easier than a normal fluid. For example, since polymers are strongly bonded in long chains, the shape of individual monomers becomes unimportant on long time scales. In simple fluids, geometrical effect associated with the shape of the molecules strongly affects the behavior. With polymers, the knowledge of just a few properties such as stiffness and size allow us to accurately discern many thermodynamic properties. This inherent simplicity is exploited to develop applications for use in industry.

One way of describing a polymer is with the number of monomers a polymer possess. The number of monomers (N) forming a polymer molecule ranges from just a few monomers to over one million monomers. Typically, the topology of a polymer are linear, ring and branched polymers to name but a few. But in this paper the topology of the polymer considered is a linear polymer. A DNA molecule is considered a polymer with

four different types of monomer units that coalesce into a very specific structure (double helix). Polymers whose monomers are identical are termed homopolymers while a polymer that has at least two different monomers is called a heteropolymer.

The shape of a polymer molecule is the first step in understanding its behavior. The typical conformation of a linear polymer is much like a random walk, each monomer positioned randomly in sequence. Several models were developed to study the shape and size of linear polymers such as the freely jointed chain [14]. These models mirror the concept that a polymer is shaped using random walk statistics but fail to account for the physical dimensions of the individual monomers. This is known as the excluded volume effect. Simply put, a monomer cannot occupy the same physical space as another monomer. Taking the excluded volume into account will cause the molecule or conformation to be larger than predicted by random walk models. This is called the swelling of the polymer chain.

Although we are interested on the dynamical properties it is important to control the static ones so there are two properties by which the spatial size of a polymer is characterized. The first is the mean end-to-end distance $\langle R^2(N) \rangle$, where \vec{R} is simply the (vector) distance between the first and last monomer and the brackets depict an ensemble average. So, the end-to-end distance describes the static property of the polymer, and this can be put mathematically as:

$$\langle R^2(N) \rangle = \langle (\vec{r}_1 - \vec{r}_N)^2 \rangle \quad (1.2.1)$$

where $\vec{r}_1 - \vec{r}_N$ is the distance between the first and last monomer of the chain.

Another method is the molecule's mean radius of gyration $\langle R_g^2(N) \rangle$, which is an average of every monomers' square distance from the polymers' center of mass, mathematically defined by [14]:

$$\langle R_g^2(N) \rangle = \frac{1}{N} \left\langle \sum_{i=1}^N (\vec{r}_i - \vec{r}_{cm})^2 \right\rangle \quad (1.2.2)$$

with

$$\vec{r}_{cm} = \frac{1}{N} \sum_{i=1}^N \vec{r}_i \quad (1.2.3)$$

Where \vec{r}_i and \vec{r}_{cm} are the position of the i^{th} monomer and the position of the polymer's center of mass, respectively. The values of $\langle R_g^2(N) \rangle$ and $\langle R^2(N) \rangle$ will be a function of the number and size of monomers.

After finding the static properties of polymers it is especially interesting to check the chain dynamics. Since the chain cannot entangle, the reptation model certainly is not an appropriate description. On the other hand in order to move around the chains as well as the monomers have to get along each other. This puts strong constraints onto the motions of the individual monomers. However, how does this affect the overall dynamical behavior?

To investigate these questions, we first analyze the mean-square displacement averaged over N monomers. Mainly, we are interested in three quantities:

$$g_1(t) = \frac{1}{N} \sum_{i=1}^N \langle (\vec{r}_i(t) - \vec{r}_i(0))^2 \rangle, \quad (1.2.4)$$

$$g_2(t) = \frac{1}{N} \sum_{i=1}^N \langle [(\vec{r}_i(t) - \vec{r}_{cm}(t)) - (\vec{r}_i(0) - \vec{r}_{cm}(0))]^2 \rangle, \quad (1.2.5)$$

$$g_3(t) = \langle (\vec{r}_{cm}(t) - \vec{r}_{cm}(0))^2 \rangle. \quad (1.2.6)$$

Where $g_1(t)$ is the mean-square displacement of the monomers, $g_2(t)$ is the mean-square displacement of the monomers relative to the center of mass and $g_3(t)$ describes the diffusion of the overall system or the mean-square displacement of the center of mass of the system.

Since polymers are very complicated topological objects, computer simulations often are the best tool to get precise theoretical information on the proposed model. For

the subsequent discussion we confine ourselves to Monte Carlo methods. Nevertheless molecular dynamic methods are very important for specific applications [15]. The Monte Carlo methods themselves can be separated into two major groups. The first are static or quasi-static methods. Here chains are generated by a certain algorithm, and information on static properties is deduced. These methods provide high accuracy data for static properties but do not allow for any dynamic interpretation [16].

Here we are interested in a dynamic algorithm that allows for the analysis of dynamic properties of polymers. This itself might be of no special interest since many lattice algorithms that obey Rouse dynamics [17-20] are given in the literature. The Rouse model describes the motion of a polymer by the Brownian dynamics of monomer of a polymer chain.

It is logical that the mean-square displacement of a polymer molecule will be quite different than that of a single particle. The Rouse model [14] was developed to describe the dynamics of a polymer molecule in solution. It is a bead-spring model that replaces solvent interactions with a friction force, and simulates the movement of the monomers using a stochastic force f_{sto} . The model considers neither hydrodynamic interactions nor the excluded volume effect. The resulting equation of motion is called the Langevin equation and it can be solved using simple mathematics. The Rouse model predicts that the mean-square displacement $\langle r^2 \rangle$ of the molecule's center of mass in 2D is:

$$\langle r^2 \rangle = \frac{4k_B T t}{N \xi}, \quad (1.2.7)$$

Where k_B is Boltzmann's constant, T is the temperature, ξ is the friction coefficient of one monomer and N is the number of monomers. Substituting the mean-square displacement $\langle r^2 \rangle = 4Dt$ in to equation 1.2.7 we have for the free solution diffusion constant:

$$D_o = \frac{k_B T}{N \xi} \quad (1.2.8)$$

or,

$$D_o \propto N^{-1} \quad (1.2.9)$$

This model does not correspond well to experimental results since hydrodynamic interactions are not taken into consideration. Nevertheless, the Rouse model is still very important and has served as the basis of numerous theoretical investigations of polymer dynamics in solutions [14]. Since our model also disregards hydrodynamic interactions, we will be using the Rouse predictions to test our models validity. It is also important to note that the Rouse model was intended for very long chains where the end effects imposed by the first and last monomers can be neglected.

Of course, polymer dynamics may deviate from Rouse predictions depending on the environment. For example, in a polymer melt, linear polymers will typically diffuse along their backbone. Because of the high density of polymers, transverse diffusion is inhibited. This type of movement is dubbed reptation and the restriction imposed on the polymers degree of freedom will of course decrease the diffusion coefficient of the polymer. The diffusion coefficient of a polymer chain undergoing reptation [14] scales to the order of $D \propto \frac{1}{N^2}$.

Another example of an environment affecting diffusion is a polymer chain inside a gel. Polymers and particles alike may then exhibit anomalous diffusion due to the disordered nature of the gel-like structure. In other words, molecular displacement may scale as: $\langle r^2 \rangle \propto t^{2/d_w}$, where $d_w > 2$, which does not correspond to normal diffusion. It is often believed that the "anomalous" diffusion of particles in gels is due to the fractal nature of the gel although there are no firm indications that the gels are indeed fractal [21]. A safer statement would be that the anomalous diffusion of molecules is linked with the level of disorder in the gel. The disorder will cause the chain to be trapped in certain areas and flow freely where there is more available free volume. These are but two common examples of situations where the diffusion of molecules may not correspond to Rouse dynamics. Since molecules invariably diffuse in nonhomogeneous solutions, these special

cases are truly relevant.

It is quite astounding that with these simple concepts of polymers such as shape and movement, described using only basic mathematics and physics, we can predict the behavior of polymers in very complex systems. These basic building blocks will allow a better comprehension throughout this work.

Chapter 2

Methods

2.1 Particle diffusion

In order to illustrate anomalous diffusion in crowded media we perform simulation using a Monte Carlo algorithm on a two-dimensional square and hexagonal lattice. Diffusion calculations are carried out first by preparing a 256 x 256 square and hexagonal lattice. A tracer is placed at the origin of the lattice and obstacles are placed at random at a prescribed concentration excluding the origin which is occupied by the tracer. In doing this no two obstacles are allowed to occupy the same lattice site. In this case only point obstacles are used for this particular simulation. And the tracer carries out a random walk on unobstructed nearest-neighbor lattice sites. A jump by a tracer may be blocked by an obstacle while it executes a random walk. Which means that the tracer have four directions to jump on a square lattice and among the four it chooses randomly one at each Monte Carlo time step to jump to the nearest-neighbor sites. If the particular lattice site is occupied by an obstacle the move will be rejected else if the site is free the move will be accepted. Similar procedure is followed for the case of hexagonal lattice except that the number of jumping directions of the tracer here is changed to six. For both of these lattice types this is clearly illustrated in figures 2.1 and 2.2.

When the tracer executes a random walk it may jump out of the box. This is because of lattice sites at the edge of our two dimensional square lattice for example has only

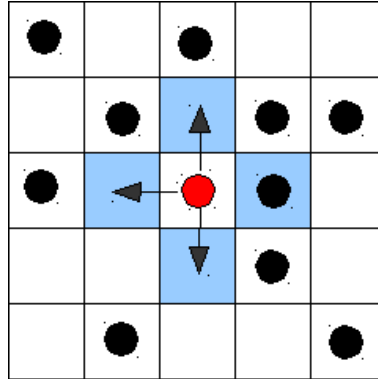


Figure 2.1: Square lattice: among the four nearest-neighbor sites the possible jump directions of the tracer (red) is indicated by the arrows (i.e up,down and left). To the right it is not possible for the tracer to jump because it is occupied by an obstacle (black).

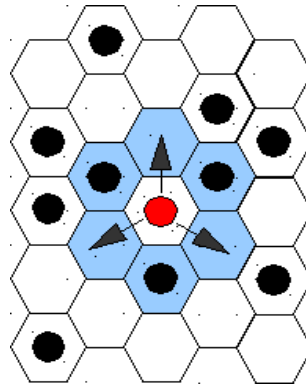


Figure 2.2: Hexagonal lattice: a single lattice site having six nearest-neighbors. The tracer at the center (red) only jumps to three free lattice sites as indicated by the arrows. Since the rest are blocked by the point obstacles (black).

three nearest neighbors ,or two if they are at the corner as compared to four neighbors for the interior lattice sites. Hence, it is important in our simulations to minimize the effects of the edges as much as possible. So one way to control this is to use an appropriate boundary condition which is called a periodic boundary condition. Now we assume that a tracer at the edge also jumps to the opposite edge of the lattice, as indicated in fig. 2.3 by the dotted lines that wrap around the lattice. A tracer which comes out at the bottom of the lattice is returned at the top. And a tracer which comes at the left of the lattice is also returned on the right side of the lattice as indicated. Alternatively we could imagine that our lattice is situated on a torus so that these "edge" sites are really neighbors of

each other. In either case we have, in a sense, eliminated all of the edge sites. Every site now has four nearest-neighbors so that all sites are in equivalent locations. The use of periodic boundary conditions thus allows us to largely circumvent boundary effects.

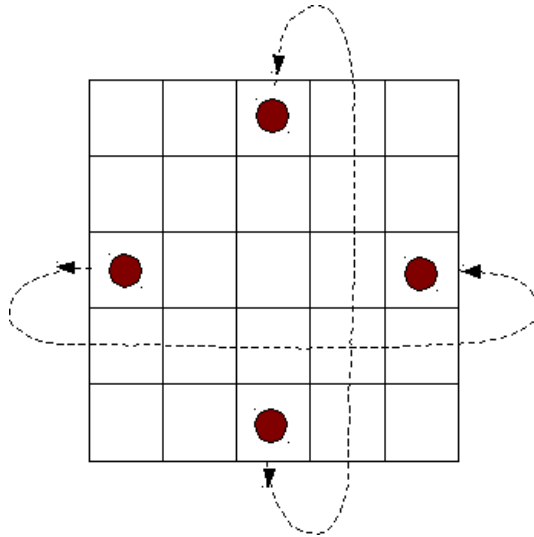


Figure 2.3: Diffusion of a tracer with periodic boundary conditions. Sites that are connected by the dotted lines that wrap around the lattice are considered to be nearest neighbors and thus a tracer can jump to the opposite edge of the lattice.

The position of the tracer is recorded as a function of time if its initial position is at the origin, which is given by the expression:

$$r_i^2(t) = x_i^2(t) + y_i^2(t), \quad (2.1.1)$$

Where $x_i(t)$ and $y_i(t)$ are the x and y coordinate of the tracer at any Monte Carlo time step respectively.

The mean-square displacement $\langle r^2 \rangle$ is obtained by averaging the positions over different random walks, which is given by:

$$\langle r^2(t) \rangle = \frac{1}{N_p} \sum_{i=1}^{N_p} (x_i^2(t) + y_i^2(t)) \quad (2.1.2)$$

Where N_p is the total number of tracers considered in the simulation.

In the simulation we use 2000 particles (tracers). Each particle executes a random walk independently with the same and different configuration of point obstacles. Typically, 50 different obstacle configurations were used, and 2000 random walks per obstacle configuration. In each run, 1000 Monte Carlo time steps were used.

The logarithm of the mean-square displacement ($\log(\langle r^2 \rangle)$) as a function of Monte Carlo time step ($\log t$) plotted for different concentration of obstacles starting from $C = 0.0$ up to $C = 0.6$ concentration for a tracer diffusing on a square lattice. The slope of the graph is the diffusion coefficient (D). And the value of the diffusion coefficient is different for the given different concentration of obstacles ranging between zero and one. To see the dependence of the diffusion coefficient on the concentration of the obstacles (C), we plot the diffusion coefficient as a function of the concentration gradient. The short time and the long time diffusion is seen by plotting $\log(\langle r^2/t \rangle)$ versus $\log t$.

2.2 Polymer diffusion

Several models for the simulation of polymers already exist. We require a model that properly simulates both the static and dynamic properties of polymers. Additionally, we want a lattice description that allows for the simulation of two dimensional polymers. The goals of this project is to study linear polymers. In order to investigate the dynamical properties of a 2D polymer system by means of Monte Carlo simulation, we have to assert that the algorithm displays Rouse dynamics for the non reversal random walk or self-avoiding walk (SAW) [16]. This random walk assert that consecutive monomers are not allowed to share the same (single) lattice site. Besides this short ranged repulsion along the chains no additional interaction is taken into account. For such a system one can use the complete set of moves as for chains with full excluded volume. This then gives a good and dependable check on the static and dynamic properties of an algorithm. For dynamic Monte Carlo algorithms the typical requirements for the moves

are, that they create new bond vectors within the chain but the number of monomers (bonds) has to be fixed. Standard lattice methods for two dimension only create new bond vectors at the ends, which then diffuse into the chain. This enhances the relaxation time artificially. To overcome this problem the bond fluctuation method (BFM) was introduced [22], which allows a variable bond length between monomers. It combines the advantage of a lattice simulation which means e.g. fast algorithms on both scalar and vector machines, with continuum approaches, so that new bond vectors are created in successful moves. This model was selected because it represents a self-avoiding walk and the simulation algorithm is ergodic in two and three dimensions. The model exhibits proper Rouse dynamics and the radius of gyration scales according to the Flory exponent exhibiting proper static properties. Moreover, the variable bond length increases the realism of the macromolecule being studied. Although initially devised with linear polymers in mind the BFM can be used to study other types of molecules such as ring and branched polymers. For completeness, the model will be briefly described. Refer to [22] for a more detailed description and analysis of this lattice model.

The BFM can be used in both two and three dimensional studies. The percept of the model is that the bond length between two connected monomers is variable. In two-dimensions, a maximum bond length, l is restricted to be $l \geq \sqrt{13}$ between two connected monomers. This restriction was necessary to avoid bond cutting. Furthermore, the minimum distance between any two monomers is $l = 2$. In between l can have the values $\sqrt{5}$, $\sqrt{8}$, 3, and $\sqrt{10}$. This fulfills our excluded volume requirement since this restriction ensures that two monomers do not occupy sites adjacent to one another. Since we look for dynamic properties $l^2 \geq 13$ guarantees that bonds never cut through each other during the course of the simulation if we start with a configuration that is self-avoiding and has no bond cuts. Figure 2.4 shows two-dimensional system based on the BFM.

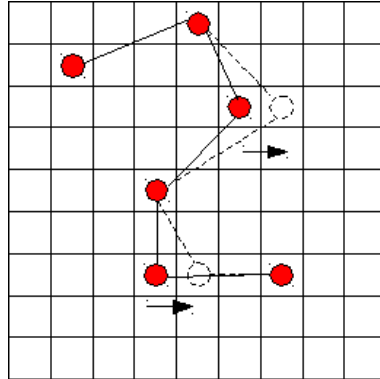


Figure 2.4: Illustration of the bond fluctuation method. The typical moves are indicated. The bond length l varies between 2 and $\sqrt{13}$. From the diagram we can see from left to right the distance between the first and the second is $\sqrt{10}$ and if we continue up to the last (six) monomers respectively we have the distances $\sqrt{5}$, $\sqrt{8}$, 2 and 3.

If the polymer consist of N monomers each monomer occupies a single site and each lattice site can only be part of one monomer (SAW condition). To move a chain, a monomer is selected at random. Then it tries to jump at random a distance of one lattice unit into one of the four (two-dimensional) lattice directions. If the move complies with both the bond length restriction and excluded volume restriction (SAW condition), the move is accepted and otherwise rejected. This leads to a natural time scale of one attempted move per monomer of the system. One can also choose another shape of the monomer. This gives only another average bond length and another bond length restriction.

Chapter 3

Results and discussion

3.1 Particle diffusion

3.1.1 Plots of mean-square displacement

If the mean-square displacement is plotted as a function of time (Fig. 3.1), the curves appear to be linear.

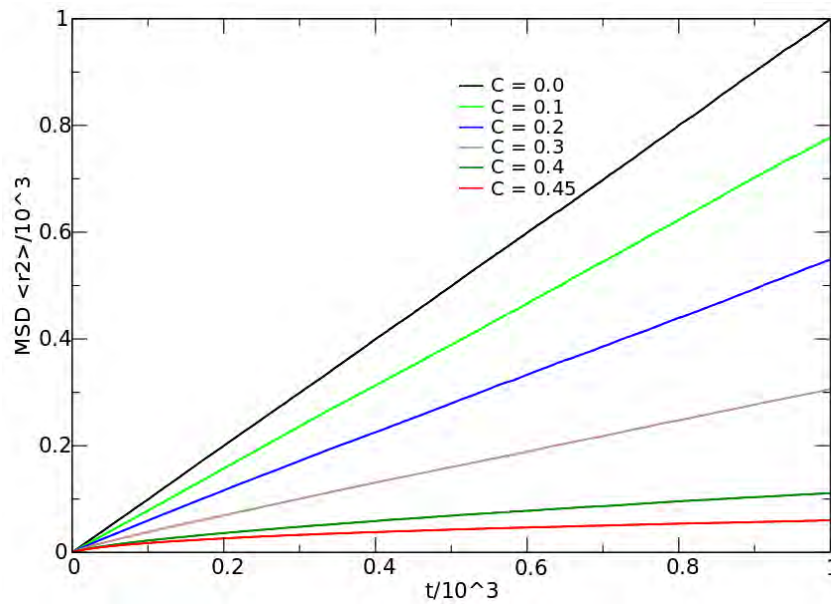


Figure 3.1: Mean-square displacement $\langle r^2 \rangle$ as a function of time t for diffusion of a point tracer on a square lattice in the presence of point obstacles at the indicated obstacle concentrations C .

From this we can clearly see that as the obstacle concentration increases, the slope decreases, yielding the usual decrease in diffusion coefficient (D) with concentration of obstacles (C). For zero concentration of obstacles ($C=0.0$) the slope of the graph is one which, implies normal diffusion. In unobstructed diffusion the mean-square displacement of the diffusing particle is proportional to time. But if the concentration of the obstacles is varied from $C = 0.1$ up to $C = 0.45$ the value of the slope of the graph starts to decrease below one. So from this result we can easily understand that obstruction affects the diffusion of a particle and the value of the diffusion coefficient decreases as the complexity of the medium increases. The same result is obtained by (Saxton,1994).

To test anomalous diffusion, the data can be re-plotted as $\log(\langle r^2 \rangle)$ versus $\log t$ as shown in (Fig. 3.2) below.

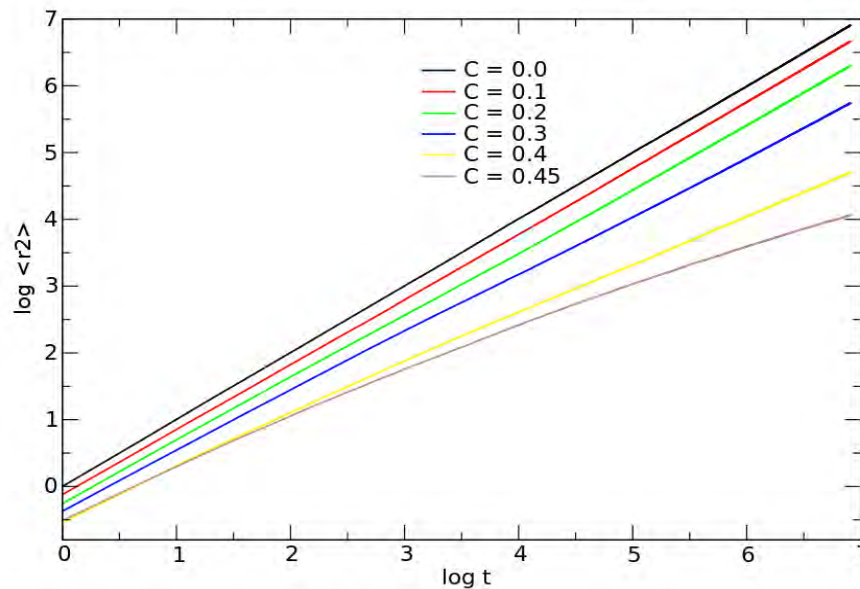


Figure 3.2: The same data re-plotted as the logarithm of the means-quare displacement $\log(\langle r^2 \rangle)$ as a function of the logarithm of time $\log t$. Again, the slight change in slope with time is evident for $C \geq 0.3$.

Normal diffusion yields a slope of one for zero concentration of obstacles. In terms of the anomalous diffusion exponent (d_w) the slope of normal diffusion can be written as $2/d_w = 1$, where $d_w = 2/D$. For a concentration gradient above $C = 0.0$ anomalous

diffusion is observed with a slope of $2/d_w \leq 1$, since $d_w \geq 2$. This result agrees with experimental finding in which single particle tracking experiment have provided evidence of anomalous diffusion of membrane protein in cells (Ghosh and Webb, 1990; Ghosh, 1991). This means that for anomalous diffusion the slope is less than one since the diffusion exponent is always greater than two. A small change in slope with time can be seen for $C \geq 0.3$. To obtain a clear picture of the time dependence, we remove the linear dependence and plot $\log(\langle r^2 \rangle / t)$ as a function of $\log t$ and this is illustrated below (Fig. 3.3). Then normal diffusion yields a line of slope zero, and anomalous diffusion yields a line of slope $(2/d_w) - 1$ which is a negative slope since d_w is always greater than two for anomalous diffusion. At short times, diffusion is anomalous; at long times, diffusion is normal below the percolation threshold. The crossover from anomalous to normal diffusion occurs at a crossover time t_{CR} ; the corresponding crossover distance is

$$R_{CR} = \sqrt{D(C, \infty)t_{CR}} \quad (3.1.1)$$

where $D(C, \infty)$ is the limiting value of $\langle r^2 \rangle / t$ for large t .

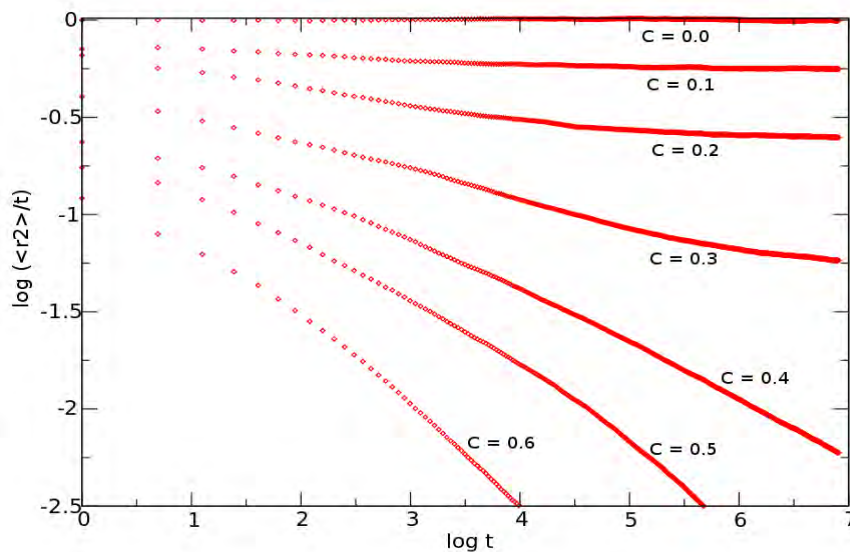


Figure 3.3: Diffusion of the tracer on a 2D square lattice in which the same data re-plotted as $\log \langle r^2 \rangle / t$ as a function of $\log t$ to obtain the clear picture of time dependence.

At the percolation threshold ($C = 0.4$) diffusion is anomalous for all times. Above the percolation threshold ($C = 0.5, 0.6$) diffusion is anomalous for short times; the limiting behavior for large times is discussed later in (Sec.3.1.2).

For the case of a tracer diffusion on a hexagonal lattice similar result is obtained (Fig. 3.4). For example when the short time and long time diffusion is obtained by plotting $\log\langle r^2 \rangle/t$ versus $\log t$, normal diffusion yields a line of slope zero, and anomalous diffusion yields a line of slope $(2/d_w) - 1$. At short times, diffusion is also anomalous; at long times, diffusion is normal below the percolation threshold. But in this case the percolation threshold is ($C = 0.6$) which is different from ($C = 0.4$) obtained for a tracer diffusing on a square lattice. Similarly for hexagonal lattice at the percolation threshold diffusion is anomalous for all times. Above the percolation threshold $C = 0.7, 0.8$ diffusion is anomalous for short times.

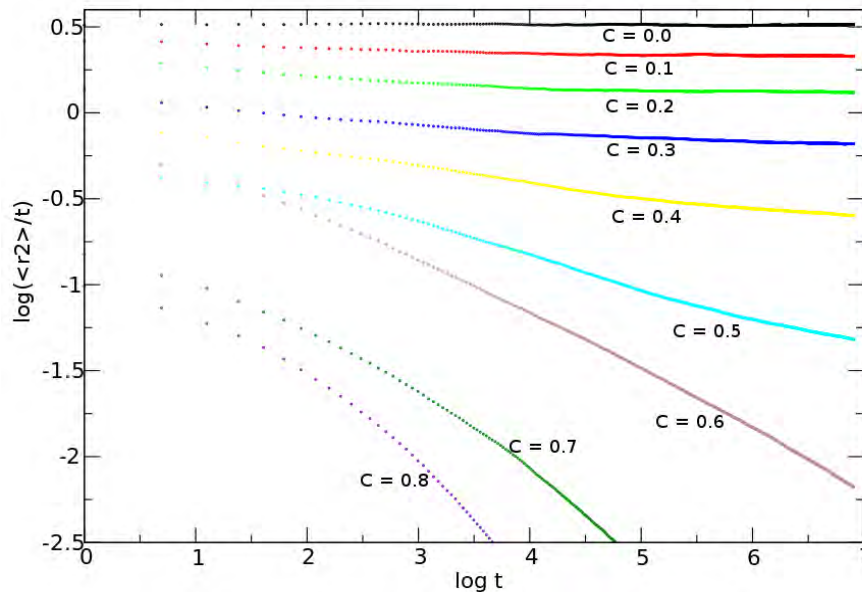


Figure 3.4: Diffusion of a tracer on a 2D hexagonal lattice which shows the time dependence of diffusion when $\log\langle r^2 \rangle/t$ as a function of $\log t$ is plotted. The percolation threshold is 0.6 in which diffusion is anomalous for all times.

3.1.2 The concentration dependence of d_w

The anomalous diffusion exponent measures the deviation from normal diffusion. Fig. 3.5 shows anomalous diffusion exponent (d_w), as a function of obstacles concentration. For a particle diffusing on a square lattice, the curve shows (square dots on the curve) the diffusion exponent is 2 for normal diffusion at $C = 0$ and it increases as the concentration increases at the percolation threshold $d_w = 2.87$ for particles diffusing on the infinite cluster (Havlin and Bunde,1991). The curves for both square and hexagonal lattices goes to this limit at the appropriate percolation threshold. At $C = 0$, diffusion is normal and $d_w = 2$; at the percolation threshold C_p , $d_w = 2.87$ for particles diffusing on the infinite cluster (Havlin and Bunde, 1991). The curve goes to this limit at the appropriate percolation threshold.

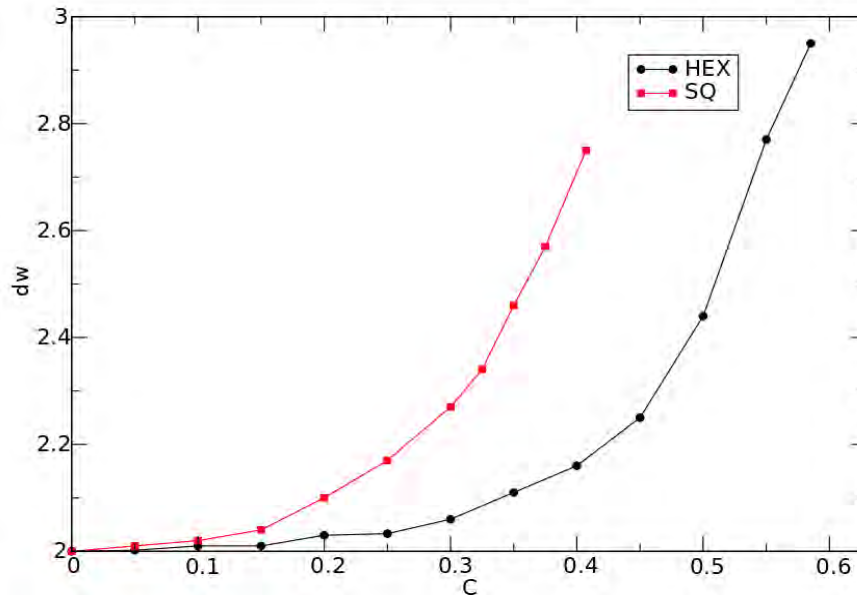


Figure 3.5: Anomalous diffusion exponent d_w as a function of obstacle concentration C for two different geometries: point obstacles on the square lattice (SQ) and point obstacles on a hexagonal lattice (HEX). At the percolation threshold $C = C_p$. Where $C_p = 0.4$ for square lattice and $C_p = 0.6$ for hexagonal lattice.

The data is re-plotted as a function of C/C_p , as shown in Fig. 3.6. The anomalous diffusion exponent as a function of the ratio of the concentration gradients below the percolation threshold (C) to the concentration gradient at the percolation threshold (C_p) for both the square and hexagonal lattices, the data falls on the same curve. This curve tells us that even if the lattice geometries are different they have the same result irrespective of their percolation threshold. Near the percolation threshold, some diffusing particles are trapped in bounded regions; well above the percolation threshold, all the diffusing particles are trapped. The bounded regions grow smaller as the obstacle concentration increases. For trapped particles, as $t \rightarrow \infty$, $\langle r^2 \rangle$ approaches a constant value proportional to the average size of the bounded regions, so the slope of $\log(\langle r^2 \rangle)$ versus $\log t$ approaches -1 (Fig. 3.3, $C = 0.5, 0.6$), and $d_w \rightarrow \infty$.

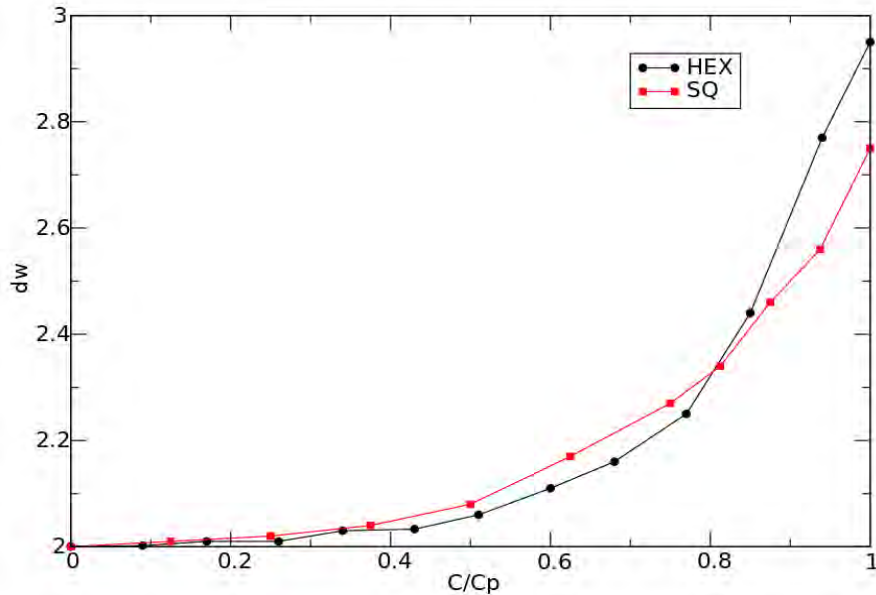


Figure 3.6: Anomalous diffusion exponent as a function of C/C_p , the value of the percolation threshold is $C_p = 0.4$ for square lattice and $C_p = 0.6$ for hexagonal lattice.

3.1.3 The concentration dependence of D

Finally, we consider the limiting value of the diffusion coefficient, D for large times. Values of D are shown as a function of obstacle concentration C in figure 3.7 for a square lattice.

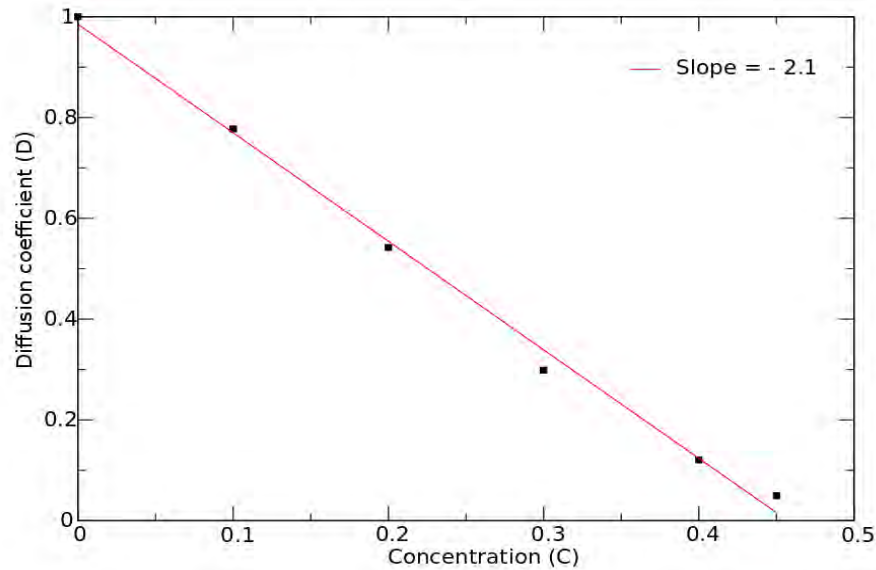


Figure 3.7: Diffusion coefficients D as a function of obstacle concentration C for point obstacles on the square lattice.

A simple least-squares fit of a straight line to $\langle r^2 \rangle$ versus t (Fig. 3.1) gives values of D . In other words it is the slope of the line obtained from the graph of $\langle r^2 \rangle$ versus t . In the least-squares the y-intercept is a free parameter. For a square lattice the concentration is varied from zero up to a little bit above the percolation threshold as shown in (Fig.3.1). The slope of the lines gives different values for the different concentrations of obstacles on a square lattice. The slope of the line is clearly the value of the diffusion coefficient. In which the value of the slope (the diffusion coefficient) varies between zero and one i.e one for zero concentration of obstacles and approaches zero as the obstacle concentration approaches one. The result is illustrated in Fig. 3.7. And the slope of the line obtained from this graph is -2.1.

3.2 Polymer diffusion

3.2.1 Static properties

Plot of end-to-end distance

To describe the configuration of a polymer we have to know the location in space of each monomer. The simplest measure of chain configuration is the mean-square end-to-end distance $\langle R^2(N) \rangle$. If the mean-square end-to-end distance is plotted as a function of the number of monomers (Fig. 3.8), the curve appears to be linear.

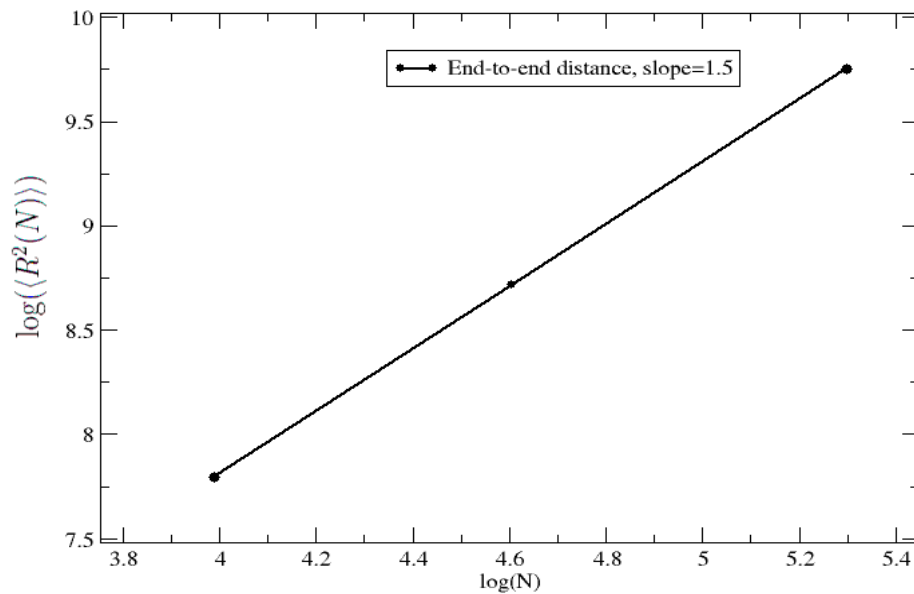


Figure 3.8: Log-log plot of end-to-end distance $\langle R^2(N) \rangle$ versus chain length N for self-avoiding walk, $\langle R^2(N) \rangle \propto N^{3/2}$. The chain length or the number of monomer considered are $N = 54, 100, 200$.

This plot is obtained for three different number of monomers $N = 54, 100, 200$ for a self-avoiding walk, in which the chain bonds are not allowed to cross each other. Here the end-to-end distance describes the static property of the polymer, which is proportional to some power of the number of monomers N .

A real polymer chain can be characterized as a self-avoiding random walk, i.e. a random walk that does not visit the same point more than once. A detailed analysis of real polymer chains was carried out by Flory [24]. Flory calculated configurations of real polymers based on the idea that their size is governed by two competing interactions. On the one hand, steric repulsion is responsible for polymer swelling. On the other hand, chain connectivity creates an attraction counteracting monomer departure. Flory combined both interactions and derived a single parameter, ν , which summarizes the net interaction between monomers. An important result from Flory's theory for a polymer in good solvent is that it yields an universal power-law dependence of polymer size R on the number of monomers N , i.e.

$$R^2 \propto N^{2\nu} \quad (3.2.1)$$

with

$$\nu = \frac{3}{2+d} \quad (3.2.2)$$

In contrast to ideal chains, the scaling behavior of the polymer size now exhibits a dependence on the dimension of space d in which the polymer resides. For a polymer in two dimension the Flory exponent becomes $\nu = 3/4$ yielding $R^2 \propto N^{3/2}$. For self-avoiding walk the simulation result showed the exponent 1.5 is clearly exhibited as expected, which can be seen from the slope of the graph shown in Fig. 3.8.

Plot of radius of gyration

In addition to the end-to-end distance the configuration of a polymer can be described by a more precise characteristic, the radius of gyration $\langle R_g^2(N) \rangle$, which uses more than the end monomers.

The radius of gyration is also plotted as a function of the number of monomers for self-avoiding walk using three different chain length $N = 54, 100, 200$ as it is shown in figure 3.9. As expected the radius of gyration is also proportional to the number of monomers

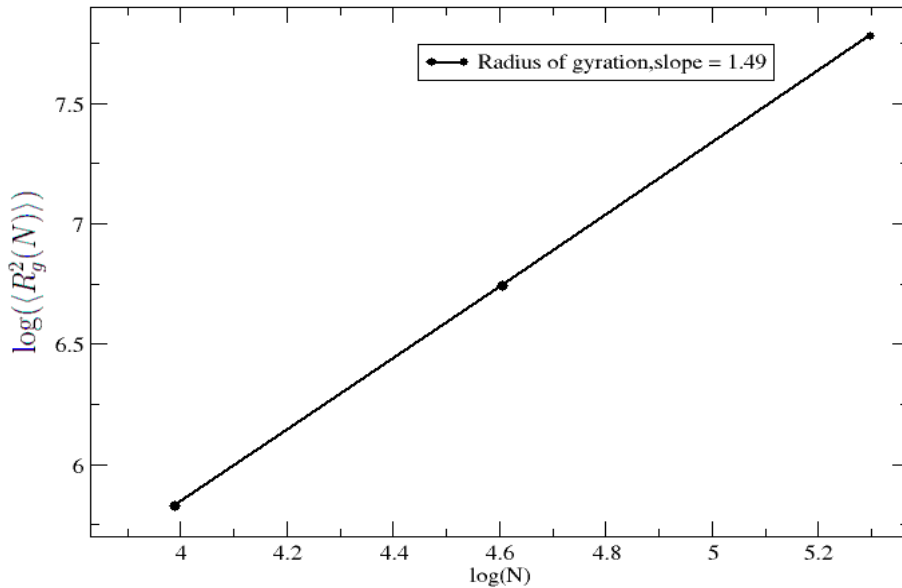


Figure 3.9: Log-log plot of radius of gyration $\langle R_g^2(N) \rangle$ versus chain length N for a self-avoiding walk, $\langle R_g^2(N) \rangle \propto N^{3/2}$. The chain length or the number of monomer considered are $N = 54, 100, 200$.

by an exponent equal to 1.5 which is obtained from the slope of the graph of the radius of gyration versus the number of monomers.

3.2.2 Dynamic properties

After finding the static properties of polymers, it is specially interesting to check the chain dynamics. We first analyze the mean-square displacement of the center of mass $g_3(t) = \langle (\vec{r}_{cm}(t) - \vec{r}_{cm}(0))^2 \rangle$, of the polymer for two different concentration of obstacles (i.e, $C=0$ and $C=0.35$). The mean-square displacement of the center of mass describes the diffusion of the overall system. Figure 3.10 shows, $g_3(t)$ as a function of Monte Carlo time step for a chain length of $N = 20, 50, 100$ with (a) zero concentration of obstacles and (b) 0.35 concentration of obstacles distributed randomly on the lattice. This result shows how the dynamics of a polymer is affected by the nature of the medium. In

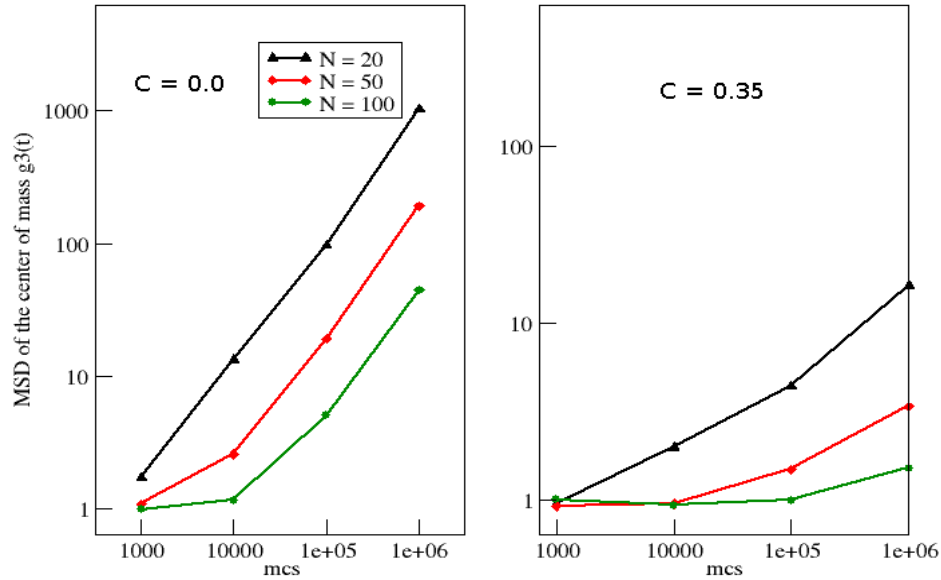


Figure 3.10: Plot of the mean-square displacement of the center of mass of a polymer $g_3(t)$ as a function of Monte Carlo time steps (a) for $C = 0.0$ and (b) for $C=0.35$ concentration of obstacles.

unobstructed diffusion (a) the mean-square displacement of the center of mass of the polymer is larger than that of obstructed diffusion (b). This tells us that obstruction hinders the diffusion of a polymer. In this case anomalous diffusion occurs, in which the mean-square displacement of the polymer is proportional to some fractional power of time.

We can see the dependence of $g_3(t)$ on concentration of obstacles between $C = 0$ and $C = 0.7$. Figure 3.11 shows $g_3(t)$ versus Monte carlo time steps for different concentration gradient. The mean-square displacement of the center of mass of the polymer decreases as the concentration of obstacles increases and approaches a constant value just above a concentration of $C = 0.4$.

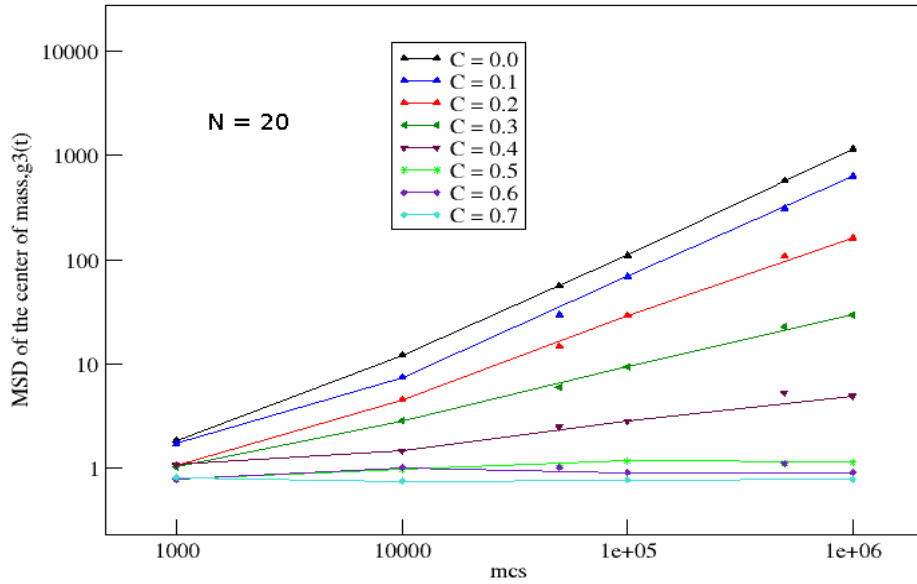


Figure 3.11: Plot of the mean-square displacement of the center of mass of a polymer $g_3(t)$ as a function of Monte Carlo time steps for a concentrations between $C = 0.0$ and $C = 0.7$.

For large time we can calculate the diffusion coefficient of a polymer diffusing in a random medium by considering a chain length of $N = 20$ monomers for different concentration of obstacles. And we can see how the diffusion constant depends on the increase in concentration of obstacles. Figure 3.12 shows the diffusion coefficient $D = \lim_{t \rightarrow \infty} (g_3(t)/t)$ as a function of concentration gradient.

The graph of diffusion constant versus concentration gradient shows that as the concentration gradient increases the diffusion constant decreases. Simply put as the medium gets crowder and crowder the polymer will be trapped in bounded regions and unable to diffuse freely through the medium. This leads the mean-square displacement of the center of mass to approach a constant value and the slope of the line obtained from the approaches to zero.

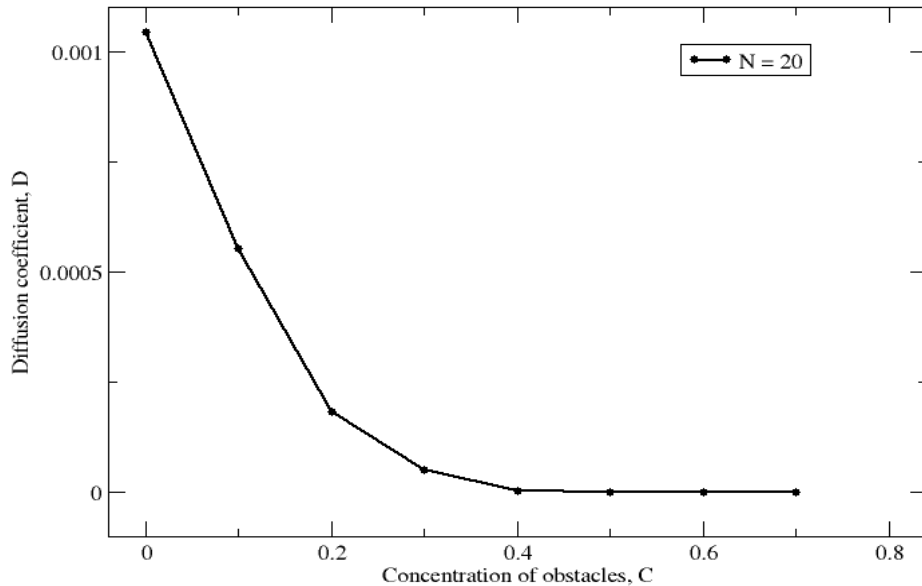


Figure 3.12: Diffusion coefficient $D = \lim_{t \rightarrow \infty} g_3(t)/t$ as a function of obstacle concentration for a chain length of $N = 20$ monomers.

The diffusion coefficient can also be investigated as a function of the number of monomers. This result is illustrated in the figure 3.13 shown below for zero concentration of obstacles. What is surprising is that the diffusion constant seems to display a weaker N -dependence than the Rouse model suggests. In Rouse model the diffusion coefficient is inversely proportional to the number of monomers ($D \propto N^{-1}$).

The mean-square displacement averaged over all monomers $g_1(t) = \frac{1}{N} \sum_{i=1}^N \langle (\vec{r}_i(t) - \vec{r}_i(0))^2 \rangle$ and $g_2(t) = \frac{1}{N} \sum_{i=1}^N \langle [(\vec{r}_i(t) - \vec{r}_{cm}(t)) - (\vec{r}_i(0) - \vec{r}_{cm}(0))]^2 \rangle$, and the mean-square displacement of the center of mass $g_3(t)$ plotted as a function of Monte Carlo time step (Fig.3.14) to test for the short time and long time diffusion of a polymer on a free lattice and on a lattice with concentration of $C = 0.2$ for a chain length of $N = 20$. At short times the mean-square displacement of the monomers $g_1(t)$ and the mean-square displacement of the monomers relative to the center of mass $g_2(t)$ exhibit the same behavior up to the longest relaxation time of the chain. After that time the diffusion of the whole chain $g_3(t)$

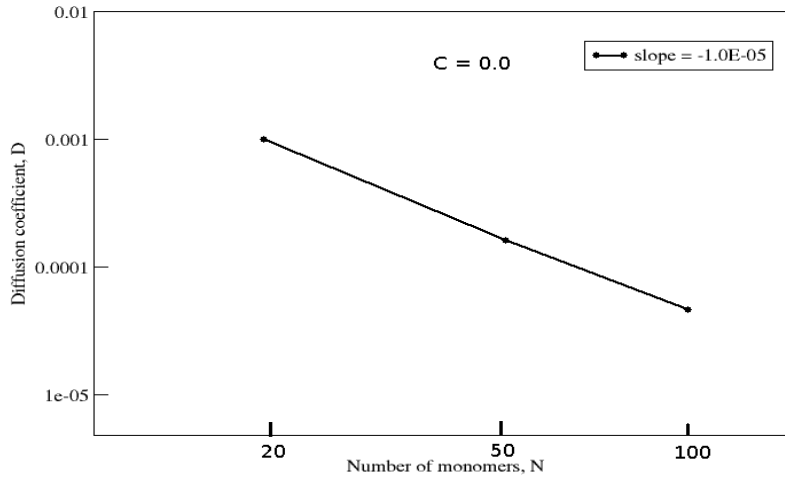


Figure 3.13: Diffusion coefficient $D = \lim_{t \rightarrow \infty} g_3(t)/t$ versus number of monomers $N = 20, 50, 100$ for zero concentration of obstacles.

takes over. We can also see from this graph that for different concentration of obstacles $g_2(t)$ saturates with different relaxation times. For the polymer diffusing on a free lattice (Fig 3.14 (a)) the relaxation time is less than that of the polymer diffusing in a disorder medium with concentration gradient $C = 0.2$ (Fig 3.14 (b)). The reason for this is that for a disordered medium the polymer will be trapped in bounded regions and needs more time $g_2(t)$ to reach its relaxation time than a free medium.

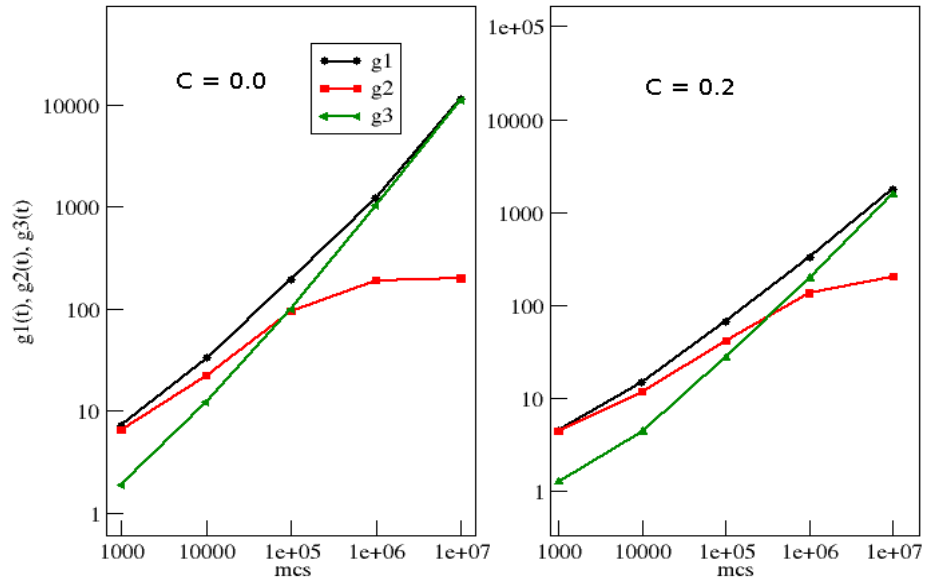


Figure 3.14: Mean-square displacement $g_1(t)$ and $g_2(t)$ and the diffusion of the center of mass of the polymer $g_3(t)$ (a) for $C = 0.0$ and (b) for $C = 0.2$ and $N = 20$ as a function of Monte Carlo time step. For calculation of this point 100 independent runs are taken into account.

Chapter 4

Summary and conclusion

We have seen how obstruction and complexity around particles can produce marked slowing of diffusion as well as anomalous diffusion. For unobstructed (normal) diffusion the mean square displacement is proportional to time and the diffusion coefficient is one. But as the concentration (C) of the obstacles increases the diffusion coefficient (D) decreases linearly, and C and D are inversely related.

For disordered systems diffusion is anomalous, and the mean-square displacement is proportional to a fractional power of time not equal to one. A log-log plot of the mean square displacement as a function of time showed anomalous diffusion, and transitions between anomalous and normal diffusion were observed at moderate concentration below the percolation threshold for both square and hexagonal lattice, $C = 0.4$ and $C = 0.6$ respectively. For $\log(\langle r^2 \rangle / t)$ versus $\log t$ normal diffusion yields a line of slope zero and anomalous diffusion yields a line of slope less than zero, which is a negative slope. Below the percolation threshold diffusion is anomalous for short times and normal for long times. In the short time regime, we found that the mean-square displacement $\langle r^2 \rangle$ is not a linear function of time because the particle has not had sufficient opportunity to fully explore its surroundings. The phenomenon is even more pronounced when the particle moves in a fractal environment. This is rarely a typical experimental situation, however, since the fractal nature of all real systems are limited both at the small and large length scales. At percolation threshold diffusion is anomalous for both short and long times or it is

anomalous at all times. Above the percolation threshold diffusion is anomalous for short times but for long times, as $t \rightarrow \infty$, $\langle r^2 \rangle$ approaches a constant value proportional to the average size of the bounded regions, so the slope of $\log(\langle r^2 \rangle/t)$ versus $\log t$ approaches -1 . Anomalous diffusion can also be characterized by the anomalous diffusion exponent d_w and the limiting diffusion coefficient D . As the concentration of obstacles increases to the percolation threshold, d_w , varies smoothly between the known limiting values for normal diffusion and percolation. The parameters are approximately independent of the lattice when plotted as a function of the appropriate concentration variable.

We presented the study of the properties of a polymer chain in a two-dimensional random media. For dynamical simulation of polymers we used a Monte Carlo algorithm. Due to the concept of fluctuating bond length, it has the advantage of giving realistic (Rouse) dynamics. By the use of the bond fluctuation method we were able to study both static and dynamic properties of the chains.

For static properties we found that the chains, although they cannot cross each other, display typical random walk behavior for quantities like mean-square end-to-end distance ($\langle R^2(N) \rangle$) and radius of gyration ($\langle R_g^2(N) \rangle$). Both the end-to-end distance and the radius of gyration are proportional to the number of monomers to the power $3/2$. This result agrees with the exponent predicted by Flory for real chains.

The most unexpected result were found for the dynamical properties. The Rouse model does not consider any other interaction between the monomers than the chain connectivity. There is no sign of decrease of mobility due to topological constraints. On the other hand the mobility of the polymer is affected by the concentration of the obstacles. At short times the mean-square displacement of the monomers $g_1(t)$ and the mean-square displacement of the monomers relative to the center of mass $g_2(t)$ exhibit the same behavior up to the longest relaxation time of the chain. After that time the diffusion of the whole chain $g_3(t)$ and the mean-square displacement of the monomers show similar behavior.

Bibliography

- [1] S. Havlin and D. Ben-Avraham, *Adv. Phys.* 51, 187 (2002).
- [2] J.P. Bouchaud and A. Georges, *Phys. Rep.* 195, 127 (1990).
- [3] H.L. Martinez, *J. Chem. Phys.* 104, 2692 (1996).
- [4] P.M. Richards, *Phys. Rev. B* 16, 1393 (1977).
- [5] V.A. Ivanov, B. Jung, A.N. Semenov, I.A. Nyrkova, and A.R. Khokhlov, *J. Chem. Phys.* 104, 4214 (1996).
- [6] A. Milchev, V. Pereyra, and V. Fleurov, *Langmuir* 10, 4698 (1994).
- [7] I. Avramov, A. Milchev, E. Arapaki, and P. Argyrakis, *Phys. Rev. E* 50, 4636 (1994).
- [8] Crank J. 1975. *The Mathematics of Diffusion*. Oxford: Oxford Univ. Press
- [9] Hines AL, Maddox RN. 1984. *Mass Transfer: Fundamentals and Applications*. Englewood Cliffs, NJ: Prentice Hall
- [10] Einstein A. 1955. *Investigations on the Theory of the Brownian Movement*. Mineola, NY: Dover
- [11] Haw MD. 2002. Colloidal suspensions, Brownian motion, molecular reality: a short history. *J. Phys. Condens. Matter* 14:776979
- [12] Metzler R, Klafter J. 2000. The random walks guide to anomalous diffusion: a fractional dynamics approach. *Phys. Rep. Rev. Sec. Phys. Lett.* 339:177
- [13] Goodsell DS. 2005. Visual methods from atoms to cells. *Structure* 13:34754
- [14]. Doi. M., Edwards S. F., *The theory of Polymer Dynamics*, Clarendon Press, Oxford 1986
- [15] Grest, G.S.; Kremer, K. *Phys. Rev. A* 1986, 33, 3628 and references therein.
- [16] Kremer, K.; Binder, K., *Comp. Phys. Rept.* 7 (1988) 259
- [17] Baumgartner, A.; Binder, K. *J. Chem. Phys.* 1979, 71, 2541.

- [18] Kremer, K.; Binder, K.; Baumgartner, A. *J. phys. A* 1982, 15, 2879. Kremer, K. *Macromolecules* 1983, 16, 1632.
- [19] Dial, M.; Crabb, K. S.; Crabb, C. C.; Kovac, J. *Macromolecules* 1985, 18, 2215.
- [20] Downey, J. P.; Crabb, C. C.; Kovac, J. *Macromolecules* 1986, 19, 2202.
- [21] Starchev, K., Sturm, J., Weill, G., Brogren, C.H., *Journal of Physical Chemistry B*, 1997, 101, 56595663
- [22] Carmesin I., Kremer K., *Macromolecules* 1988, 21, 28192823
- [23] Nienhuis, B. *Phys. Rev. Lett.* 1982, 49, 1062.
- [24] Flory P. The configuration of real polymer chains. *J Chem Phys*, 17, p. 303, 1949.

Declaration

This thesis is my original work, has not been presented for a degree in any other University and that all the sources of material used for the thesis have been dully acknowledged.

Name: Solomon Negash

Signature:

Place and time of submission: Addis Ababa University, June 2010

This thesis has been submitted for examination with my approval as University advisor.

Name: Dr. Tatek Yergou

Signature: